

1 **Big data managing in a landslide Early Warning System: experience from a ground-based**  
2 **interferometric radar application**

3 Emanuele Intrieri<sup>1</sup>, Federica Bardi<sup>1</sup>, Riccardo Fanti<sup>1</sup>, Giovanni Gigli<sup>1</sup>, Francesco Fidolini<sup>2</sup>, Nicola  
4 Casagli<sup>1</sup>, Sandra Costanzo<sup>3</sup>, Antonio Raffo<sup>3</sup>, Giuseppe Di Massa<sup>3</sup>, Giovanna Capparelli<sup>3</sup>, Pasquale  
5 Versace<sup>3</sup>.

6 <sup>1</sup> Department of Earth Sciences, University of Florence, via La Pira 4, 50121, Florence, Italy

7 <sup>2</sup> Pizzi Terra srl, via di Ripoli 207H, 50126, Florence, Italy

8 <sup>3</sup> Department of Soil Defense, University of Calabria, Ponte Pietro Bucci, Cube 41b, 87036,  
9 Arcavacata di Rende (CS), Italy

10

11 *Correspondence to:* Emanuele Intrieri (emanuele.intrieri@unifi.it)

12

13

14 **Keywords:** early warning system; slope instability; big data; monitoring; landslide; risk  
15 management; ground-based interferometric radar

16

17 **1 Abstract**

18 A big challenge in terms of landslide risk mitigation is represented by the increasing of the  
19 resiliency of society exposed to the risk. Among the possible strategies to reach this goal, there is  
20 the implementation of early warning systems. This paper describes a procedure to improve early  
21 warning activities in areas affected by high landslide risk, such as those classified as Critical  
22 Infrastructures for their central role in society.

23 This research is part of the project “LEWIS (Landslides Early Warning Integrated System): An  
24 Integrated System for Landslide Monitoring, Early Warning and Risk Mitigation along Lifelines”.

25 LEWIS is composed of a susceptibility assessment methodology providing information for single  
26 points and areal monitoring systems, a data transmission network and a Data Collecting and  
27 Processing Center (DCPC), where readings from all monitoring systems and mathematical models  
28 converge and which sets the basis for warning and intervention activities.

29 The aim of this paper is to show how logistic issues linked to advanced monitoring techniques such  
30 as big data transfer and storing, can be dealt with, compatibly with an early warning system.  
31 Therefore, we focus on the interaction between an areal monitoring tool (a ground-based  
32 interferometric radar) and the DCPC. By converting complex data into ASCII strings and through  
33 appropriate data cropping and average, and by implementing an algorithm for line of sight  
34 correction, we managed to reduce the data daily output without compromising the capability of  
35 performing.

36

## 37 **2 Introduction**

38 Urbanization, especially in mountain areas, can be considered a major cause for high landslide risk  
39 because of the increased exposure of elements at risk. Among the elements at risk, important  
40 communication routes, such as highways, can be classified as Critical Infrastructures (CIs), since  
41 their rupture can cause chain effects with catastrophic damages on society (Geertsema et al 2009;  
42 Kadri et al. 2014). On the other hand, modern society is more and more dependent from CIs and  
43 their continuous efficiency (Lebaka et al., 2016), and this has risen their value over the years. The  
44 result is a higher social vulnerability in the face of loss of continuous operation (Kröger, 2008). The  
45 main objective was to improve the social preparedness to the growing landslide risk, according with  
46 the suggestions of several authors (Gene Corley et al., 1998; Baldrige et al., 2011; Urlainis et al.  
47 2014; 2015). This led to the development of several approaches and frameworks for increasing the  
48 resiliency of society exposed to the risk (Kröger, 2008; Cagno et al., 2011 and references therein).  
49 The resiliency policy of course involves prevention activities but also, and more importantly, those  
50 activities needed to maintain functionality after disruption (Snyder and Burns, 2009) and to  
51 promptly alert incoming catastrophes in order to protect people and prepare for a possible damaging  
52 of the endangered CI. Among these activities, the implementation of integrated landslides early  
53 warning systems (*i.e.* LEWIS, Versace et al., 2012; Costanzo et al., 2016) reveals its increasing  
54 importance.

55 In this context, the methodology described in this paper has been conceived; it has been tested and  
56 validated on a portion of an Italian highway, affected by landslides and selected as case study: it is  
57 located in Southern Italy, along a section of the A16 highway, an important communication route  
58 that connects Naples to Bari where a ground based interferometer (GB-InSAR) has been installed  
59 on the test site, in order to obtain spatial monitoring data.

60 One of the main drawbacks of advanced instruments such as GB-InSAR is how to handle the large  
61 data flow deriving from continuous real-time monitoring. The issue is to reduce the capacity needed  
62 for analyzing, transmitting and storing big data without losing important information. The main  
63 feature of this paper is indeed the management of monitoring data in order to filter, correct, transfer  
64 and access them compatibly with the needs of an early warning system.

65

## 66 **3 Materials and methods**

### 67 *3.1 GB-InSAR*

68 The Ground-Based Interferometric Synthetic Aperture Radar (GB-InSAR) is composed of a  
69 microwave transceiver mounted on a linear rail (Tarchi et al., 1997; Rudolf et al., 1999; Tarchi et  
70 al., 1999). The system used is based on a Continuous Wave – Stepped Frequency radar, which  
71 moves along the rail at millimeter steps, in order to perform the synthetic aperture; the longer the  
72 rail the higher the cross-range resolution. The microwave transmitter produces, step-by-step,  
73 continuous waves around a central frequency, which influences the cross-range resolution and  
74 determines the interferometric sensitivity *i.e.* the minimum measurable displacement, usually  
75 largely smaller than the corresponding wavelength.

76 The radar produces complex radar images containing the information relative to both phase and  
77 amplitude of the microwave signal backscattered by the target (Bamler and Hartl, 1998; Antonello  
78 et al., 2004). The amplitude of a single image provides the radar reflectivity of the scenario at a  
79 given time, while the phase of a single image is not usable. The technique that enables to retrieve  
80 displacement information is called interferometry and requires the phase from two images. In this  
81 way, it is possible to elaborate a displacement map relative to the elapsed time between the two  
82 acquisitions.

83 The main added value of GB-InSAR is its capability of blending the boundary between mapping  
84 and monitoring, by computing 2D displacement maps in near real-time. The use of this tool to  
85 monitor structures, landslides, volcanoes, sinkholes is largely documented (Calvari et al., 2016; Di  
86 Traglia 2014; Intrieri et al., 2015; Bardi et al., 2016, 2017; Martino and Mazzanti, 2014; Severin,  
87 2014; Tapete et al., 2013), as well as for early warning and forecasting (Intrieri et al., 2012; Carlà et  
88 al., 2016a; 2016b; Lombardi et al., 2016).

89 GB-InSAR systems probably reveal their full potential in emergency conditions. They are  
90 transportable and only require from few tens of minutes to few hours to be installed (depending on  
91 the logistics of the site). Moreover, they can detect "near-real time" area displacements, without  
92 accessing the unstable area, 24h and in all weather conditions (Del Ventisette et al., 2011; Luzi,  
93 2010; Monserrat et al., 2014). On the other hand, some limitations reduce the GB-InSAR technique  
94 applicability: first of all the scenario must present specific characteristics in order to reflect  
95 microwave radiations, maintaining high coherence values (Luzi, 2010; Monserrat et al., 2014); only  
96 a component of the real displacement vector can be identified (i.e. the component parallel to the  
97 sensor's line of sight); maximum detectable velocities are connected to the time that the system  
98 needs to obtain two subsequent acquisitions. Sensors need power supply that, for long term  
99 monitoring, cannot be replaced by batteries, generators or solar panels.

100 With the specific aim of performing an early warning system, data acquired *in situ* must be sent  
101 automatically to a "control center" where they are integrated in a complete early warning system  
102 procedure (Intrieri et al., 2013). In this sense, another main limitation is represented by the necessity  
103 to transfer a high quantity of data, whose weight has to be reduced to the minimum, in order to  
104 reduce the load on transmission network.

105 The employed system is a portable device designed and implemented by the Joint Research Center  
106 (JRC) of the European Commission and its spin-off company Ellegi-LiSALab (Tarchi et al., 2003;  
107 Antonello et al., 2004).

### 108 3.2 Early warning system architecture

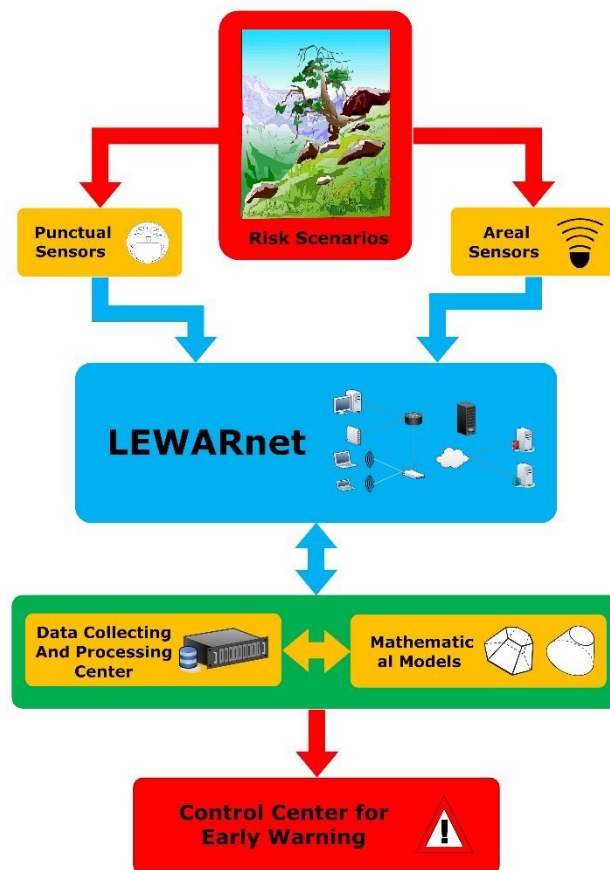
109 Morphological features, hydrogeological factors and sudden rainfall can cause diverse types of  
110 movements or fall of earthy and rock materials. The unpredictability and diversity of these events  
111 make structural interventions often inappropriate to reduce the related risk, and real-time  
112 monitoring network difficult to implement.

113 In the last decade, Wireless Sensor Networks (WSNs) have been largely used in various fields. A  
114 significant increase in the use of WSN, due to their simplicity, low cost of installation,  
115 manufacturing and maintenance, has been recorded in the framework of environmental monitoring  
116 applications (Intrieri et al., 2012; Liu et al., 2007; Yoo et al., 2007). Distinct types of sensor nodes  
117 of these networks, distributed with high density in the monitored areas, send environmental

139 information to the concentrators nodes, generating a considerable amount and a wide variety of  
140 collected data. Due to the significant growth of data volumes to be transferred, the WSN require  
141 flexible ad-hoc protocols, able to respect constraints related to energy consumption management  
142 (Hadadian and Kavian, 2016; Khaday et al., 2015; Parthasarathy et al., 2015). In particular, many  
143 protocols have been developed that offer data aggregation patterns to optimize the sensor nodes  
144 battery life (Kim et al., 2015) or sleep/measurement/data transfer cycles to minimize the energy  
145 consumption (Fei et al., 2013; Venkateswaran and Kennedy, 2013).

146 LEWIS (Costanzo et al., 2016) uses heterogeneous sensors, distributed in the risk areas, to monitor  
147 the several physical quantities related to landslides. The measured data, through a  
148 telecommunications network, flow into the Data Collecting and Processing Center (DCPC), where,  
149 using suitable mathematical models for the monitored site, the risk is evaluated and eventually the  
150 state of alert for mitigation action is released (Figure 1 Figure 1).

151 The system, through a modular architecture exploiting a telecommunication network (called  
152 LEWARnet) based on an ad-hoc communication protocol and an adaptive middleware, has a high  
153 flexibility, which allows for the use of different interchangeable technological solutions to monitor  
154 the parameters of interest.



155  
156 **Figure 1. LEWIS architecture.**

157  
158 The network has been equipped with both single point sensors as well as area sensors. The present  
159 paper addresses a sub-network comprising an area sensor, the GB-InSAR.

160 The different sensors types generate asynchronous traffic, thus imposing the adoption of an ad-hoc  
161 transmission protocol. This can support an asynchronous transmission mode to the DCPC, and it is  
162 equipped with message queues management capacity to reconstruct historical data series, between  
163 two connection sessions, in case of null or partial transmission. This operation mode requires the  
164 presence of a software architecture that operates as a buffer, acting as an intermediary or as  
165 middleware (LEWARnet), between the data consumer (DCPC) and the data producers (sensors and  
166 sub-networks of sensors).

167 The developed middleware also monitors the processes of transmission and data acquisition,  
168 recognizing the activity status of the sensors and that of the DCPC, and integrating encryption and  
169 data compression functions.

170 A detail description of LEWIS can be found in Costanzo et al. (2015; 2016).

171

### 172 *3.3 Data Collecting and Processing Center (DCPC)*

173 The management of information flows, the telematic architecture and the services for data  
174 management are entrusted to the DCPC.

175 The DCPC has been designed and performed according to a complex hardware and software  
176 system, able to ensure the reliability and continuity of the service, providing advance information of  
177 possible dangerous situations that may occur.

178 In the research project, the DCPC has to ensure the continuous exchange of information among  
179 monitoring networks, mathematical models and the Command and Control Center (CCC), that is  
180 responsible for emergency management and decision making.

181 Data flow from the monitoring network was managed according to a communication protocol,  
182 implemented by the DCPC, and named AqSERV. AqSERV was designed considering the  
183 heterogeneity of devices of monitoring and transmission networks (single point and area sensors)  
184 and the available hardware resources (microcontrollers and/or industrial computers). AqSERV was  
185 devised to link DCPC database (named LEWISDB) to the monitoring networks, after validation for  
186 the authenticity of the node that connects to the center. Data acquisition, before the storage in the  
187 database, is validated both syntactically and according to the information content. The procedures  
188 for extraction of the information content and validation have been realized differently for single  
189 point and area sensors: the latter require a more complex validation, as they work in a 2D domain.

190 The complete management of the monitoring networks by DCPC has been realized through specific  
191 remote commands, sent to individual devices via AqSERV, to reconfigure the acquisition intervals  
192 or to activate any sensor, depending on the natural phenomena occurring in real time.

193 The configuration of monitoring networks, composed by devices and sensors, of communication  
194 protocol used by each network, and of rules for extraction and validation of information content is  
195 carried out through a web application that allows for the management of the entire system by the  
196 users.

197 The real-time search for acquisitions is carried out through a WebGIS, specifically designed for  
198 WSNs, but that can be easily extended to classic monitoring networks.

199 The WebGIS was designed according to the traditional web architecture, client-server, by using  
200 network services which are web mapping oriented:

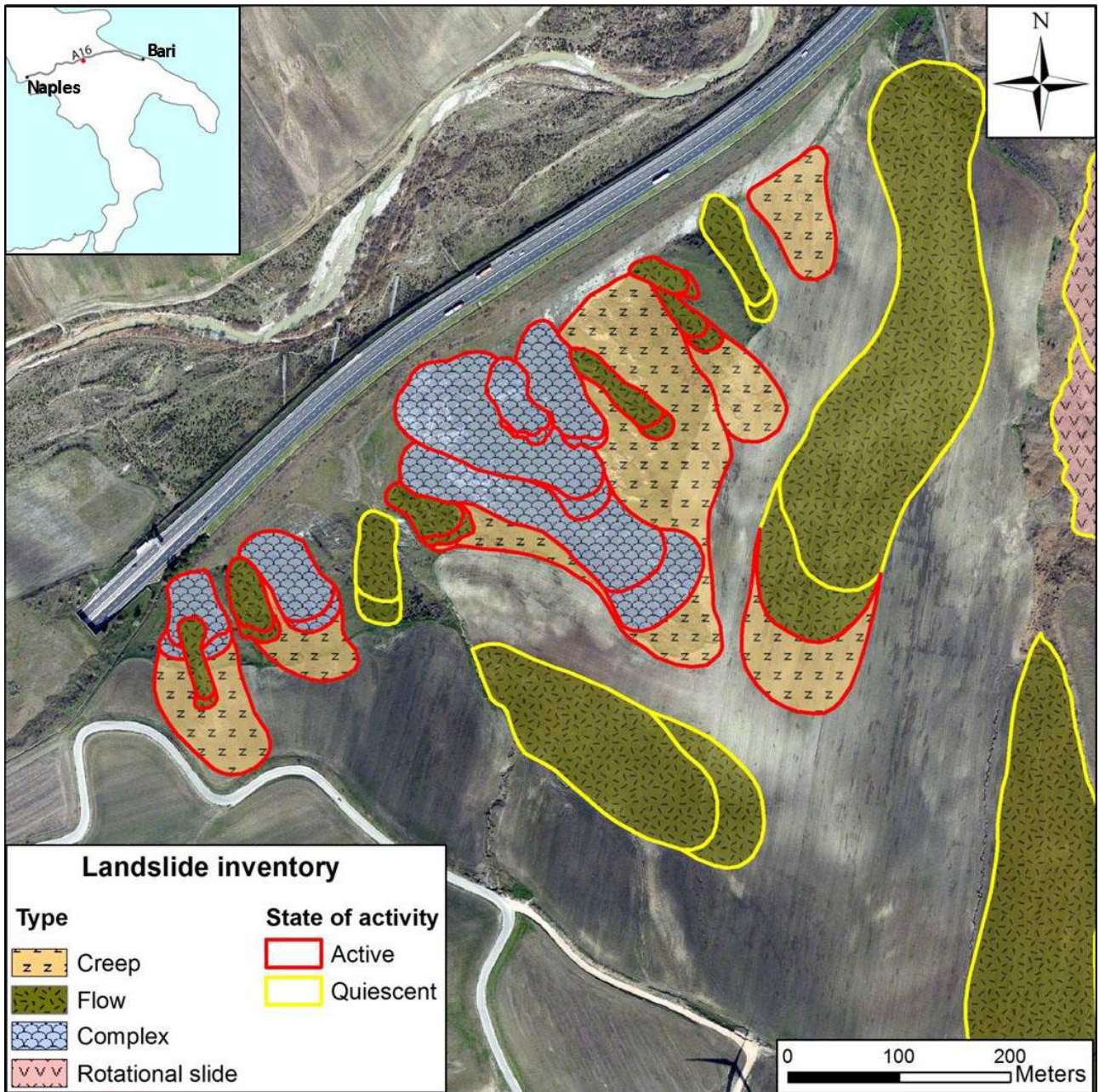
- 201 - web server for static data;
- 202 - web server for dynamic data;



- 214 - server for maps;
- 215 - database for the management of map data.
- 216

217 **4 Test site**

218 The test site chosen to experiment the integrated system is located in Southern Italy, along a section  
 219 of the A16 highway, an important communication route that connects Naples to Bari (**Figure**  
 220 **2**). The A16 selected section develops in SW-NE direction, along the Southern Italian  
 221 Apennine, in correspondence with the valley of the Calaggio Creek, between the towns of  
 222 Lacedonia (Campania Region) and Candela (Puglia Region).



223  
 224 **Figure 2. Landslides detected through field survey along the monitored section of A16 highway.**

256 The area is tectonically active, but the landscape, characterized by gentle slopes, is mostly  
257 influenced by lithologic factors rather than by tectonics. The lithologies outcropping in this area are  
258 Pliocene-Quaternary clay, clayey marlstones, and more recent (Holocene) terraced alluvial  
259 sediments (from clay to gravel). The landslides shown in [Figure 2](#) are all located in clay or  
260 clayey marlstones.

261 The highway runs on the right flank of the Calaggio Creek at an altitude between 300 and 400 m  
262 a.s.l.; the section of interest represents an element at risk in the computation of landslide risk  
263 assessment, due to the presence of unstable areas which can potentially affect the communication  
264 route ([Figure 2](#)). These unstable areas mainly involve clayey superficial layers.

265 On 1<sup>st</sup> July 2014, the GB-InSAR system was installed on the test site. The location of the  
266 installation point was selected taking into account the view of the unstable area and the distance  
267 from the power supply network. A covered structure was built to protect the system from  
268 atmospheric agents and possible acts of vandalism, in the perspective of a long-term monitoring.

269 The transmission network was provided by a GSM modem, exploiting the 3G network. In addition  
270 to the PC integrated in the GB-InSAR power base, a further external PC was exclusively employed  
271 for data post elaboration and transmission.

272 The system acquired from the beginning of July 2014 until the end of July 2015.

273 The installation location allowed the system to detect an area between 40 and 400 meters far from  
274 the its position in range direction, and about 360 m wide in the azimuth direction. These values,  
275 coupled with a 40° vertical aperture of the antennas, allowed operators to detect an area of about  
276 360 m x 360 m.

## 277 **5 Data management**

278 The most relevant matter of this monitoring was not as much related to the detection of landslide  
279 movements threatening the highway, as to how a long-term monitoring performed with an  
280 instrument providing huge amounts of data could have been run without resorting to large hard  
281 drives nor to fast internet connections. In fact, the monitoring area was covered by a 3G mobile  
282 telecommunication networks, with a limit of 2 gigabyte data transfer per month and there was the  
283 need to reduce the massive data flow produced by the radar.

284 For this reason, an appropriate data management ([Figure 3](#)) was developed and is here  
285 described.

286

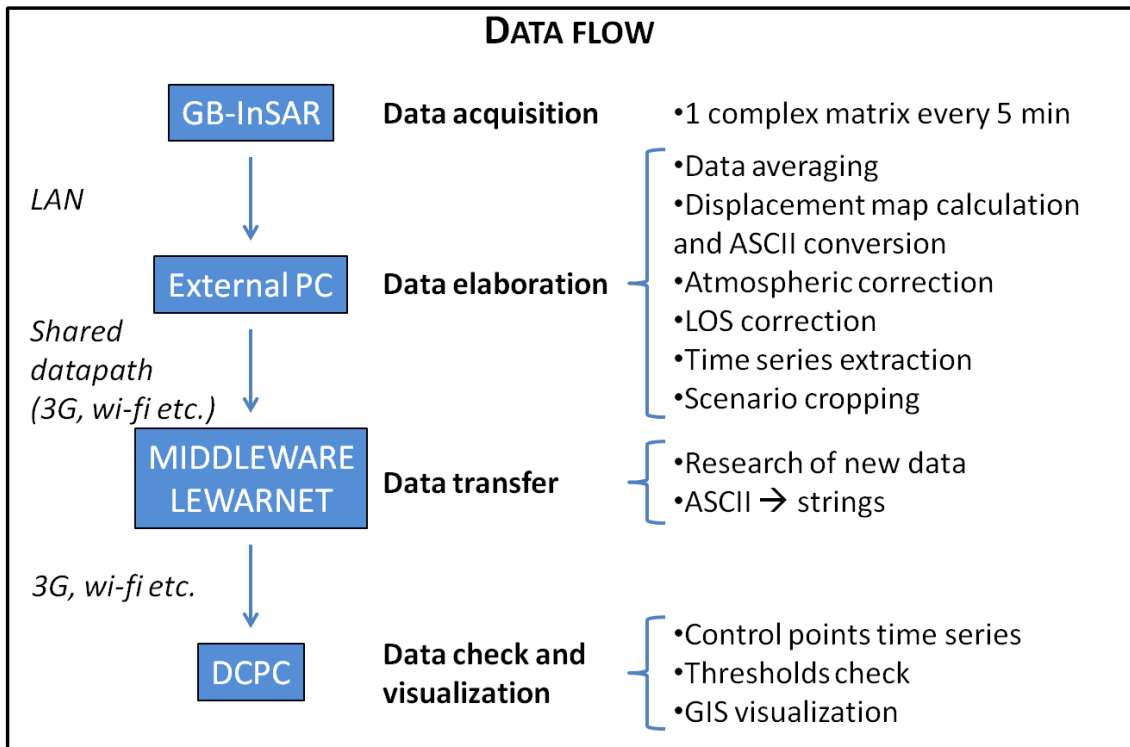


**Figure 35.** Diagram showing the complete data flow from acquisition to final visualization.

287  
288

### 289 5.1 Data acquisition

290 The GB-InSAR employed produced a single radar image, consisting in a 1001x1001 complex  
291 matrix, every 5 minutes. Each one is around 8 Megabytes large, resulting in more than 2 Gigabytes  
292 of data produced every day.

293 This amount of data represented an issue for both store capacity and data transmission.

### 294 5.2 Data elaboration

295 After being acquired, data were then transferred through LAN connection to the external PC  
296 implementing a dedicated Matlab script locally performing the actions described as follows.

#### 297 5.2.1 Data averaging

298 In order to reduce the noise normally affecting radar data (especially in vegetated areas), the images  
299 acquired every 5 minutes were also averaged using all data of the previous 8 and 24 hours. Then  
300 images averaged on 24 hours have been used to calculate daily displacement maps, every 8 hours to  
301 create 8h displacement maps and non-averaged images to calculate 5 minutes displacement maps.  
302 These time frames have been selected based on the characteristics of the slope movements and  
303 signal/noise ratio in the investigated area.

304 Averaging is also a mean to make a good use of a high data frequency, since it enables to reduce the  
305 memory occupied in the database as an alternative to their direct elimination.



333 5.2.2 Displacement map calculation and ASCII conversion

334 Each radar image can be represented as in Eq.1:

335 
$$S_n = A_n \exp(j\varphi_n) \tag{1}$$

336 where  $A_n$  is the amplitude of the  $n^{\text{th}}$  image,  $\varphi_n$  its phase and  $j = (-1)^{1/2}$  is the imaginary unit. The  
337 displacement  $\Delta r$  occurred in the time period between the acquisition of  $S_1$  and  $S_2$  has been  
338 calculated with the following (Eq.2):

339 
$$\Delta r = (\lambda/4\pi) \cdot \Delta\varphi \tag{2}$$

340 where  $\lambda$  is the wavelength of the signal and

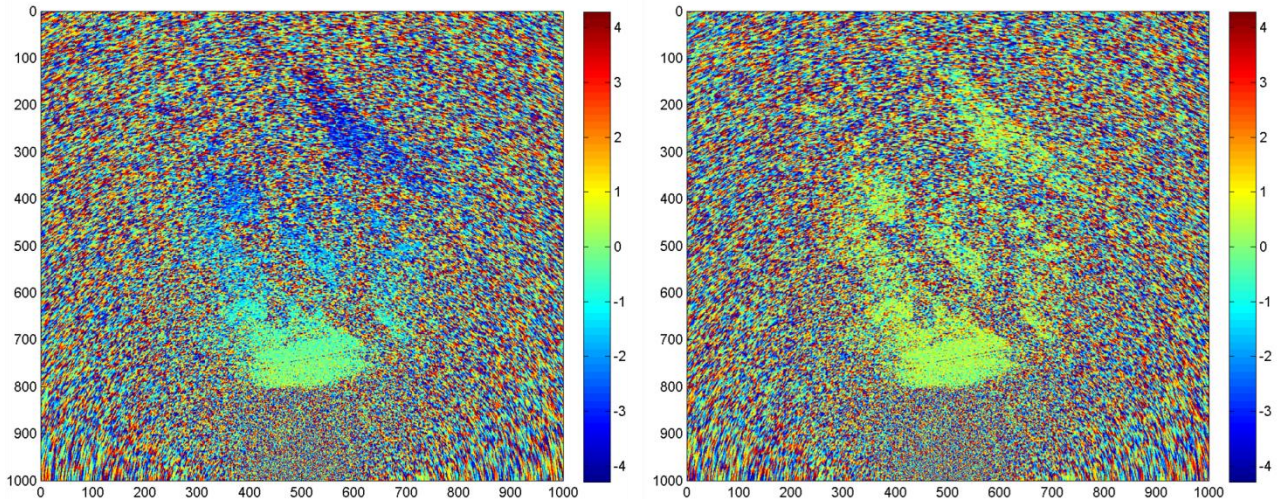
341 
$$\Delta\varphi = \varphi_1 - \varphi_2 \tag{3}$$

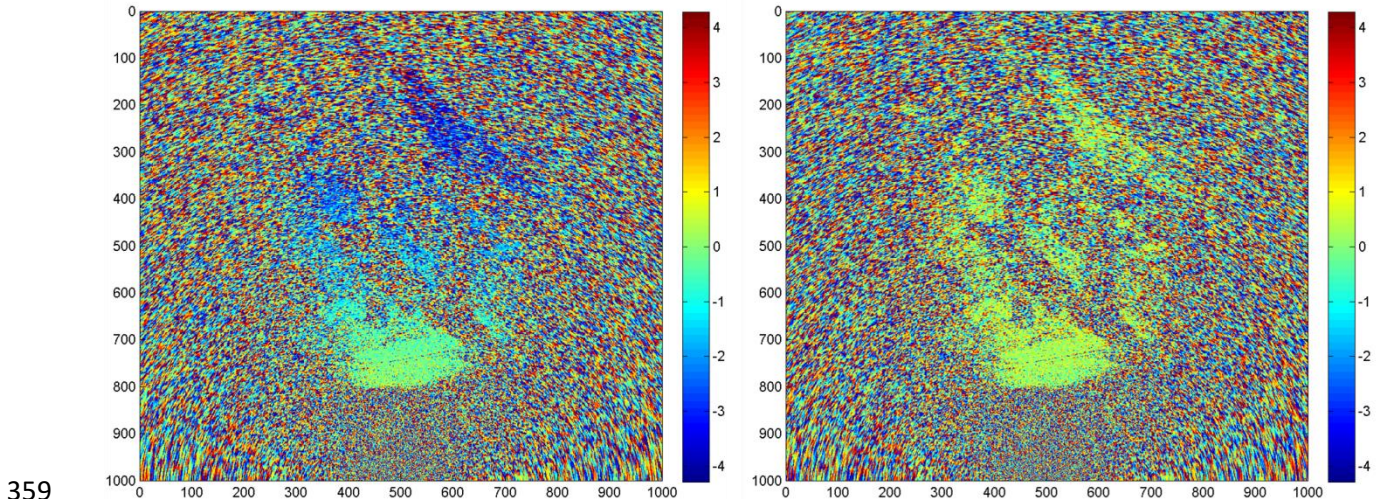
342 can be derived from:

343 
$$S_3 = S_1 S_2^* = A_1 A_2 \exp[j(\varphi_1 - \varphi_2)] \tag{4}$$

344 As a result, an ASCII file, only containing the information relative to the displacement for each  
345 pixel, was obtained.

346 5.2.3 Atmospheric correction

347 One of the major advantages of GB-InSAR is the capability to achieve sub-millimeter precision.  
348 However, this can be severely hampered by the variations of air temperature and humidity,  
349 especially when long distances are involved. Usually, atmospheric correction is performed by  
350 choosing one area considered stable, taking into account that every displacement value different  
351 from 0 is due to atmospheric noise and assuming that this offset is a linear function of the distance.  
352 Based on this relation all the displacement map is corrected. In our case the whole scenario has been  
353 selected and then only the potential unstable zones and those with a weak or incoherent  
354 backscattered signal were removed. The remaining areas were then considered stable and therefore  
355 were used for calculating the atmospheric effects. This results in a larger correction region that  
356 enables a statistical correlation between the atmospheric effects and the distance and therefore the  
357 calculation of a site-specific regression function that may not necessarily be linear (Figure 4  
358 ).



359

381 **Figure 46.** The color bar is expressed in mm; green indicates stable pixels, while blue and red  
382 respectively movement toward and away from the GB-InSAR. Left: raw interferogram showing  
383 artificial displacement increasing linearly with distance (as typical of atmospheric noise). Right: the  
384 same interferogram after the atmospheric correction.

#### 385 5.2.4 Line of sight correction

386 The availability to detect only the LOS (Line Of Sight) component of the displacement vector  
387 represents one of the main limitations of the GB-InSAR technique. A method to partially overcome  
388 this limitation has been applied in this paper, following the procedure described in Colesanti &  
389 Wasowski, 2006 and later in Bardi et al. 2014 and 2016. Other methods have been employed by  
390 Cascini et al. (2010; 2013).

391 Assuming the downslope direction as the most probable displacement path, radar data have been  
392 projected on this direction. Input data as the angular values of *Aspect* and *Slope* have been derived  
393 from the *Digital Terrain Model* (DTM) of the investigated area; furthermore, azimuth angle and  
394 incidence angle of the radar LOS have been obtained.

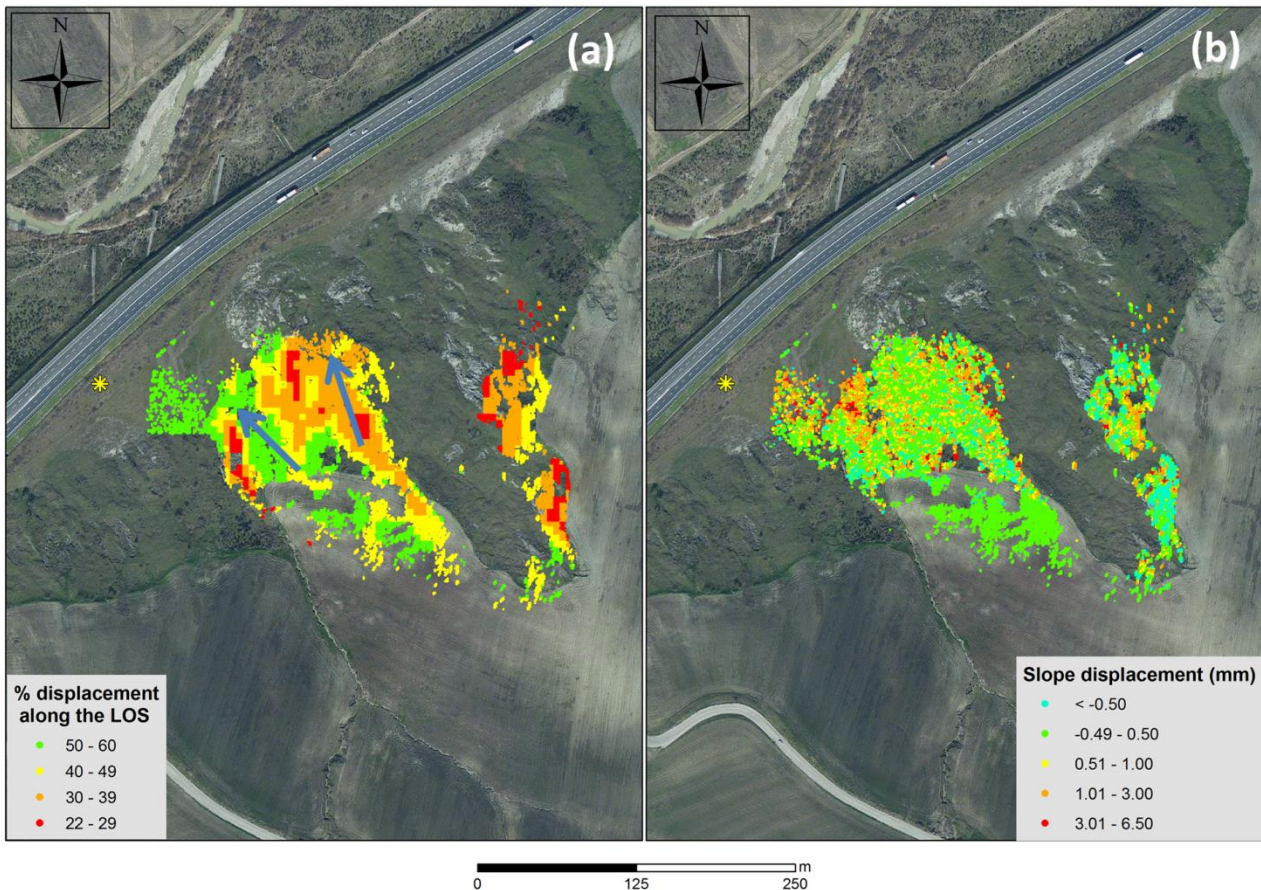
395 After calculating the direction cosines of LOS and Slope (respectively functions of azimuth and  
396 incidence angles and aspect and slope angles) in the directions of Zenith ( $Z_{los}$ ,  $Z_{slope}$ ), North ( $N_{los}$ ,  
397  $N_{slope}$ ) and East ( $E_{los}$ ,  $E_{slope}$ ), the coefficient  $C$  is defined as follow (Eq. 5):

$$398 \quad C = Z_{los} \times Z_{slope} + N_{los} \times N_{slope} + E_{los} \times E_{slope} \quad (5)$$

399  $C$  represents the percentage of real displacement detected by the radar sensor (Figure 5Figure 7A).

400 The real displacement ( $D_{real}$ ) is defined as the ratio between the displacement recorded along the  
401 LOS ( $D_{los}$ ) and the  $C$  value (Figure 5Figure 7 B).





421

422 **Figure 57.** (a) *C* values map. Blue arrows indicate the downslope direction. (b) Cumulated  
 423 displacement values projected along the downslope direction, referred to a period between 1 July 2014  
 424 and 1 November 2014. The yellow asterisk in the left of the images represents the location of the GB-  
 425 InSAR.

426 Assuming that the studied landslide actually moves along the downslope direction, the GB-InSAR  
 427 detectable real displacement percentage ranges between 22 and 60 % (Figure 5Figure-7A).

428 In Figure 5Figure-7B, an example of slope displacement map has been shown. Here, cumulated  
 429 displacement data related to a period between 1 July and 1 November 2014 have been projected  
 430 along the downslope direction. Data show as the area can be considered stable in the referred  
 431 period; maximum displacement values of 4 mm in 4 months (eastern portion of observed scenario)  
 432 can be still considered in the range of stability.

### 433 5.2.5 Time series extraction

434 In order to allow for a fast data transfer and velocity threshold comparison, some representative  
 435 control points were selected, aimed at providing cumulated displacement time series. Control points  
 436 were retrieved from the same displacement maps calculated as described in paragraph 5.2.25.2.2  
 437 and therefore can be relative to a time frame of 5 minutes, 8 hours or 24 hours.

438 In case of noisy data, instead of having a time series relative to a single pixel, these can be retrieved  
 439 from a spatial average obtained from a small area consisting of few pixels.

#### 440 5.2.6 Scenario cropping

441 Typically, the field of view of a GB-InSAR is larger than the actual area to be monitored. In fact, a  
442 portion of the radar image may be relative to the ground, sky, areas geometrically shadowed or  
443 covered by dense vegetation. These may be of no interest or even containing no information at all.  
444 For the case here studied around 50% of a radar image had a low coherence and was for all practical  
445 purposes, unusable. Therefore, a cropping of the ASCII displacement map occurred in order to  
446 frame only the relevant area.

#### 447 5.3 *Data transfer and visualization*

448 The interferometric data generated by GB-InSAR, after the pre-processing and proper correction  
449 previously described, are ready for transfer to the DCPC. The transmission of these data to the  
450 DCPC is mediated by the middleware, which interrogates the GB-InSAR for tracking the state,  
451 detects the newest data, and reorders and marks them to properly build data time series to be  
452 transferred to DCPC.

453 Subsequently, the middleware manages communications with the DCPC, according to the  
454 implemented ad-hoc protocol. This ensures the security of data providers through encrypted  
455 authentication mechanisms, it allows for recovering missing or partially transmitted data, thus  
456 avoiding information loss, and provides data acquired by the sensors to the DCPC in a standardized  
457 format, JSON, able to guarantee uniformity between the various information provided by the  
458 various sensors types. All these particular features fully justify the adoption of an ad-hoc protocol  
459 for data transfer, instead of using a standard protocol such as FTP.

460 The data files produced by the GB-InSAR have already been locally pre-processed and result in a  
461 matrix expressed in ASCII code; the dimensions of the matrix are known and range from 1x1 (for  
462 the displacement of single control points) to 1001x1001 (for uncropped displacement maps). Before  
463 encapsulating these data in the message to be transferred to DCPC, the middleware converts them  
464 from ASCII code to character strings, using the standard coding ISO / IEC 8859-1, so being able to  
465 obtain a data compression with a factor equal to  $\approx 8$ .

466 Eventually the DCPC is entrusted for cumulating the displacements relative to the control points,  
467 which are compared with the respective thresholds, and for visualizing the displacement maps as  
468 WebGIS layers, thus enabling data validation and the evaluation of the extension of moving surface.

### 469 **6 Early warning procedures discussions**

470 The GB-InSAR is part of a larger early warning system (LEWIS) which also includes other  
471 monitoring systems and simulation models. Therefore, to understand how GB-InSAR data can be  
472 used in an early warning perspective, it is necessary to make reference to LEWIS as a whole.

473 Any information, coming from the investigated sites and subsequently processed also by using the  
474 simulation models, is used to define an intervention model. This is based on the following elements:  
475 event scenarios, risk scenarios, levels of criticality, levels of alert.

476 Event scenarios describe the properties of expected phenomena in terms of dimension, velocity,  
477 involved material and occurrence probability. Occurrence probability depends on the associated  
478 time horizon, which should be equal to few hours at most, in the case of early warning systems.

505 Evaluation of occurrence probability is carried out by using information from monitoring systems  
506 and/or from outputs of adopted mathematical models for nowcasting. All the properties, to be  
507 analyzed for event scenarios, are listed below; a subdivision in classes is adopted for each one:

- 508 • landslide velocity (5 classes from slow to extremely rapid);
- 509 • landslide surface (5 classes from very small to very large);
- 510 • landslide scarp (5 classes from very small to very large);
- 511 • landslide volume (5 classes from extremely small to large);
- 512 • thickness (5 classes from very shallow to very deep);
- 513 • magnitude (3 classes: low, moderate, high), which combines the previous information;
- 514 • involved material (mud, debris, earth, rock, mixture of components);
- 515 • occurrence probability (zero, low, moderate, high, very high, equal to 1).

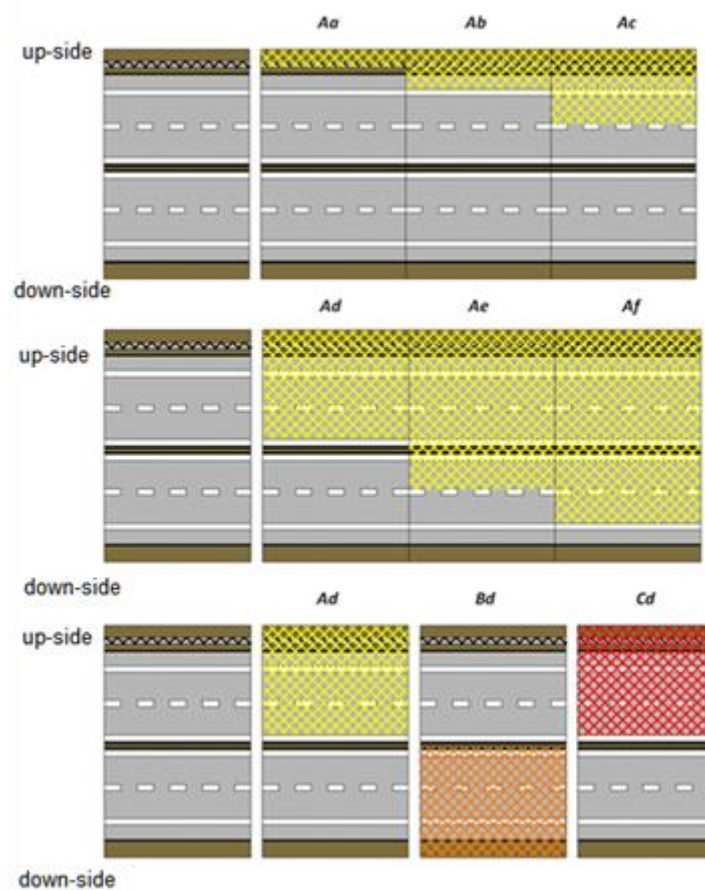
516 While some of the aforementioned parameters are determined by geological surveys, landslide  
517 velocity is directly derived from monitoring data (such as those collected by GB-InSAR). Landslide  
518 surface can be determined by geomorphological observation but is precisely quantified by GB-  
519 InSAR, thanks to its capability of producing 2D displacement maps.

520 Risk scenarios can be firstly grouped in the following three classes:

- 521 A. mud and/or debris movements which could induce a friction reduction between the vehicles  
522 and the tar and therefore facilitate slips;
- 523 B. road subsidence induced by landslides that could drag or drop vehicles;
- 524 C. falls of significant volumes and/or boulders that could crush or cover vehicles and constitute  
525 an obstacle for other vehicles.

526 For each previous risk scenario, six sub-scenarios can be identified based on the number of  
527 potentially involved infrastructures, carriageways and lanes (a. hydraulic infrastructures and/or  
528 barriers, b. only emergency lane, c. lane, d. fast lane, e. fast lane of the opposite carriageway, f. lane  
529 of the opposite carriageway). Thus, all possible risk scenarios are 18 (Figure 6Figure 8), indicated  
530 with a couple of letters (Capital and small).





531  
532  
533  
534

**Figure 68. Top and middle: possible risk scenarios involving the scenario A (landslides that could reduce friction) to increasing sectors of the highway. Bottom: combinations of scenarios with several types of phenomena (A, B, C) affect the emergency lane, lane and fast lane.**

535  
536  
537  
538  
539  
540  
541  
542

The following information is provided to DCPC:

- Measurements from sensors
  - Model outputs
- and four states are identified for each of them:
- state 0 = no variation
  - state 1 = small variation
  - state 2 = moderate variation
  - state 3 = high variation.

543  
544  
545  
546  
547

In practice, for the GB-InSAR, such states are delimited by fixed velocity values (thresholds). In this application values have been selected according to the gathered data, the first threshold being just above the instrumental noise; the remaining have been set based on expert judgement waiting for a more robust calibration, which is possible only after at least a partial mobilization of the slope. Anyway, the system is open to any method for determining thresholds (Crosta and Agliardi, 2003; Du et al., 2013; Carlà et al., 2016a) and also to the use of other parameters (acceleration for example).

550  
551

Besides information from sensors and models, other information is obtained from meteorological and hydrological models (named as indicators).

552 Indicators comprise weather forecasting and output of FLAIR and Sushi models (Sirangelo et al.  
 553 2003; Capparelli and Versace 2011) on the basis of observed and predicted (for the successive six  
 554 hours) rainfall heights.

555 Two states are defined for indicators:

- 556 • state 0 = no variation or not significant,
- 557 • state 1 = significant variation.

558 To sum up, DCPC has the following information in any moment:

- 559 ▶ state (0, 1) of indicators (IND),
  - 560 ▶ state (0, 1, 2, 3) of sensors and models running for the specific highway section (SEN),
- 561 and, on the basis of these states, four different decisions can be made by DCPC, one of which with  
 562 three options.

563 All the possible decisions are illustrated in Table 1, in which the weight of the several sensors is  
 564 assumed to be the same. Based on the notices of criticality levels provided by the DCPC, and on its  
 565 own independent evaluations, the CCC issues the appropriate warning notices (Surveillance, Alert,  
 566 Alarm and Warning) and makes decisions about the consequent actions.

567

State of sensors and/or models	DCPC decisions
All INDs and SENs are S0	0 - no decision
At least one IND is S1 and all SENs are S0	1 – SOD (Sensor On Demand) activation
At least one SEN is S1	2 – to intensify the presence up to 24 hours/day
At least $n$ SENs are S1 or at least one SEN is S2	3/1 – to issue a notice of ordinary criticality (level 1)
At least $n$ SENs are S2 or at least one SEN is S3	3/2 - to issue a notice of moderate criticality (level 2)
At least $n$ SENs are S3	3/3 - to issue a notice of high or severe criticality (level 3)

568

**Table 1. DCPC possible decisions.**

569 The information of each sensor and the results produced by the models are used to assess, in each  
 570 instant, the occurrence probability of an event scenario in the monitored areas and the possible risk  
 571 scenarios.

572 This combination of heterogeneous data was carried out by identifying for each sensor and model a  
 573 typical information (displacement, precipitation, inclination, etc.), evaluating the state in each  
 574 instant, according to a threshold system, and combining this result for all sensors placed in a  
 575 monitored geomorphological area.

576 The result is constituted by the occurrence probability of an event scenario, that is associated with a  
 577 specific action by the DCPC. In particular, if the occurrence probability is low, moderate or high it  
 578 is necessary to issue a notice of criticality (ordinary - Level 1, moderate - Level 2, High - Level 3)  
 579 to the CCC.

580 The DCPC sends two types of information:

- 581 1) criticality state of the single monitored geomorphological unit,
- 582 2) criticality state of the whole area.

583 The adopted communication protocol between the two centers for the exchange of information was  
584 carried out through a web service provided by the CCC, using the classes and attributes of the  
585 methodology named Datex II (which is a protocol for the exchange of traffic data). The use of the  
586 web service allowed to ensure the interoperability of data between the two centers, regardless of the  
587 used hardware and software architecture, through a persistent service capable of ensuring an  
588 immediate restoration of the connections, in case of malfunction and a continuous monitoring  
589 between the two centers, even in the absence of criticality.  
590

## 591 **7 Conclusions**

592 The GB-InSAR is a monitoring tool that is becoming more and more used in landslide monitoring  
593 and early warning, especially thanks to its capability of producing real-time, 2D displacement maps.  
594 On the other hand, it still suffers from some drawbacks, such as the limitation of measuring only the  
595 LOS component of a target's movement and logistic issues like those owing to a massive  
596 production of data that may cause trouble for both storing capacity and data transfer. In particular,  
597 the latter is a more and more common problem of advanced technologies that are able to produce  
598 high quality data with a high acquisition frequency, which may leave the problem of find the  
599 balancing between exploiting all the information and at the same time avoiding unnecessary  
600 redundancy.

601 These problems have been addressed when a GB-InSAR was integrated within a complex early  
602 warning system (LEWIS) and only a limited internet connection was available. This situation  
603 required that a series of pre-elaboration processes and data management procedures took place in  
604 situ, in order to produce standardized and reduced files, carrying only the information needed when  
605 it was needed. The procedures mainly concerned the transmission of data averaged over determined  
606 time frames, proportionate with the kinematics of the monitored phenomenon. Previously,  
607 transmission data were also corrected (both in terms of atmospheric noise and LOS) and reduced,  
608 by filtering out the information relative to the amplitude of the targets, by eliminating the areas not  
609 relevant for the monitoring and by transforming the matrices into strings.

610 As a result, GB-InSAR data converged into the early warning system and contributed to it by  
611 producing displacement time series of representative control points to be compared with fixed  
612 thresholds. Displacement maps were also available for data validation by expert operators and for  
613 retrieving information relative to the surface of the moving areas.

614

615 *Competing interests.* The authors declare that they have no conflict of interest.

616

617 *Acknowledgements.* This research is part of the project “LEWIS (Landslides Early Warning  
618 Integrated System): An Integrated System for Landslide Monitoring, Early Warning and Risk  
619 Mitigation along Lifelines”, financed by the Italian Ministry of Education, Universities and  
620 Research and co-funded by the European Regional Development Fund, in the framework of the  
621 National Operational Programme 2007-13 “Research and Competitiveness”, grant agreement no.  
622 PON01\_01503.

623 The Authors are thankful to Giuseppe Della Porta and his colleagues from Autostrade S.p.A. for  
624 their availability in permitting and supporting the installation and maintenance of the GB-InSAR  
625 along the A16 highway.

## 626 **References**

- 627 Antonello, G., Casagli, N., Farina, P., Leva, D., Nico, G., Sieber, A. J., Tarchi, D.: Ground-based  
628 SAR interferometry for monitoring mass movements. *Landslides*, 1 (1), 21-28, 2004
- 629 Baldridge, S.M., Marshall, J.D.: Performance of structures in the January 2010 MW 7.0 Haiti  
630 earthquake. In: *Structures Congress*, 2011. doi: 10.1061/41171(401)145
- 631 Bamler, R. and Hartl, P.: Synthetic Aperture Radar Interferometry. *Inverse Problems*, 14, R1-R54,  
632 1998.
- 633 Bardi, F., Frodella, W., Ciampalini, A., Del Ventisette, C., Gigli, G., Fanti, R., Basile, G., Moretti,  
634 S., Casagli, N.: Integration between ground based and satellite SAR data in landslide mapping: The  
635 San Fratello case study”, *Geomorphology*, 223, 45-60, 2014.
- 636 Bardi, F., Raspini, F., Ciampalini, A., Kristensen, L., Rouyet, L., Lauknes, T. R., Frauenfelder, R.  
637 & Casagli, N.: Space-Borne and Ground-Based InSAR Data Integration: The Åknes Test Site.  
638 *Remote Sensing*, 8(3), 237, 2016.
- 639 Bardi, F., Raspini, F., Frodella, W., Lombardi, L., Nocentini, M., Gigli, G., Morelli, S., Corsini, A.,  
640 Casagli, N.: Monitoring the Rapid-Moving reactivation of Earth Flows by Means of GB-InSAR:  
641 The April 2013 Capriglio Landslide (Northern Appennines, Italy). *Remote Sensing*, 9(2), 165, 2017.
- 642 Cagno, E., De Ambroggi, M., Grande, O., Trucco, T.: Risk analysis of underground infrastructures  
643 in urban areas. *Reliability Engineering & System Safety* 96, 139-148, 2011.
- 644 Calvari, S., Intrieri, E., Di Traglia, F., Bonaccorso, A., Casagli, N., Cristaldi, A.: Monitoring crater-  
645 wall collapse at active volcanoes: a study of the 12 January 2013 event at Stromboli. *Bulletin of*  
646 *Volcanology*, 78 (5), 39, 2016.
- 647 Capparelli, G., Versace, P.: FLAIR and SUSHI: Two mathematical models for early warning of  
648 landslides induced by rainfall. *Landslides*, 8 (1), 67-79, 2011.
- 649 Carlà, T., Intrieri, E., Di Traglia, F., Casagli, N.: A statistical-based approach for determining the  
650 intensity of unrest phases at Stromboli volcano (Southern Italy) using one-step-ahead forecasts of  
651 displacement time series. *Natural Hazards*, 84 (1), 669-683, 2016a.
- 652 Carlà, T., Intrieri, E., Di Traglia, F., Nolesini, T., Gigli, G., Casagli, N.: Guidelines on the use of  
653 inverse velocity method as a tool for setting alarm thresholds and forecasting landslides and  
654 structure collapses. *Landslides*, 14(2), 517-534, 2016b.
- 655 Cascini, L., Fornaro, G., Peduto, D.: Advanced low- and full-resolution DInSAR map generation  
656 for slowmoving landslide analysis at different scales. *Engineering Geology*, 112 (1-4), 29-42,  
657 doi:10.1016/j.enggeo.2010.01.003, 2010.
- 658 Cascini, L., Peduto, D., Pisciotta, G., Arena, L., Ferlisi, S., Fornaro, G.: The combination of  
659 DInSAR and facility damage data for the updating of slow-moving landslide inventory maps at

660 medium scale. *Nat. Hazards Earth Syst. Sci.*, 13, 1527-1549, doi:10.5194/nhess-13-1527-2013,  
661 2013.

662 Colesanti, C. and Wasowski, J.: Investigating landslides with space-borne Synthetic Aperture Radar  
663 (SAR) interferometry. *Eng. Geol.*, 88, 173–199, 2006.

664 Costanzo, S., Di Massa, G., Costanzo, A., Morrone, L., Raffo, A., Spadafora, F., Borgia, A.,  
665 Formetta, G., Capparelli, G., Versace, P.: Low-cost radars integrated into a landslide early warning  
666 system. *Advances in Intelligent Systems and Computing*, 354, 11-19, 2015.

667 Costanzo, S., Di Massa, G., Costanzo, A., Borgia, A., Raffo, A., Viggiani, G., Versace, P.:  
668 Software-defined radar system for landslides monitoring. *Advances in Intelligent Systems and*  
669 *Computing*, 445, 325-331, 2016.

670 Crosta, G.B., Agliardi, F.: How to obtain alert velocity thresholds for large rockslides. *Physics and*  
671 *Chemistry of the Earth, Parts A/B/C*, 27 (36), 1557-1565, 2002.

672 Del Ventisette, C., Intrieri, E., Luzi, G., Casagli, N., Fanti, R., Leva, D.: Using ground based radar  
673 interferometry during emergency: The case of the A3 motorway (Calabria Region, Italy) threatened  
674 by a landslide. *Natural Hazards and Earth System Science*, 11 (9), 2483-2495, 2011.

675 Di Traglia, F., Nolesini, T., Intrieri, E., Mugnai, F., Leva, D., Rosi, M., Casagli N.: Review of ten  
676 years of volcano deformations recorded by the ground-based InSAR monitoring system at  
677 Stromboli volcano: a tool to mitigate volcano flank dynamics and intense volcanic activity. *Earth*  
678 *Science Reviews*, 139, 317-335, 2014.

679 Du, J., Yin, K., Lacasse, S.: Displacement prediction in colluvial landslides, three Gorges reservoir,  
680 China. *Landslides*, 10 (2), 203-218, 2013

681 Fei, X., Zheng, Q., Tang, T., Wang, Y., Wang, P., Liu, W., Yang H.: A reliable transfer protocol for  
682 multi-parameter data collecting in wireless sensor networks", 2013 15<sup>th</sup> International Conference on  
683 Advanced Communication Technology: Smart Services with Internet of Things, ICACT 2013, 569-  
684 573, 2013.

685 Geertsema, M., Schwab, J.W., Blais-Stevens, A., Sakals, M.E.: Landslides impacting linear  
686 infrastructure in west central British Columbia. *Natural Hazards*, 48, 59-72, 2009.

687 Gene Corley, W., Mlakar, P.F.Sr., Sozen, M.A., Thornton, C.H.: The Oklahoma City bombing:  
688 Summary and recommendations for multihazard mitigation. *J. Perform. Constr. Facil.* 12, 100-112,  
689 1998.

690 Hadadian, H. and Kavian, Y.: Cross-layer protocol using contention mechanism for supporting big  
691 data in wireless sensor network", 2016 10<sup>th</sup> International Symposium on Communication Systems,  
692 Networks and Digital Signal Processing (CSNDSP), 2016.

693 Intrieri, E., Gigli, G., Mugnai, F., Fanti, R., Casagli, N.: Design and implementation of a landslide  
694 early warning system. *Engineering Geology*, 147-148, 124-136, 2012.

695 Intrieri, E., Gigli, G., Casagli, N., Nadim, F.: Brief communication Landslide Early Warning  
696 System: Toolbox and general concepts. *Natural Hazards and Earth System Science*, 13 (1), pp. 85-  
697 90, 2013.



698 Intrieri, E., Gigli, G., Nocentini, M., Lombardi, L., Mugnai, F., Casagli, N.: Sinkhole monitoring  
699 and early warning: An experimental and successful GB-InSAR application. *Geomorphology*, 241,  
700 304-314, 2015.

701 Kadri, F., Birregah, B., Châtelet, E.: The impact of natural disasters on critical infrastructures: A  
702 domino effect-based study. *Journal of Homeland Security and Emergency Management*, 11, 217-  
703 241, 2014.

704 Khaday, B., Matson, E. T., Springer, J., Kwon, Y.K., Kim, H., Kim, S., Kenzhebalin, D., Sukyeong,  
705 C., Yoon, J., Woo, H. S.: Wireless Sensor Network and Big Data in Cooperative Fire Security  
706 system using HARMS, 2015 6<sup>th</sup> International Conference on Automation, Robotics and  
707 Applications (ICARA), 2015.

708 Kim, Y., Bae, P., Han, J., Ko, Y.B.: Data aggregation in precision agriculture for low-power and  
709 lossy networks", 2015 IEEE Pacific Rim Conference on Communications, Computers and Signal  
710 Processing (PACRIM), 2015.

711 Kröger, W.: Critical infrastructures at risk: A need for a new conceptual approach and extended  
712 analytical tool. *Reliability Engineering & System Safety*, 93, 1781-1787, 2008.

713 Labaka, L., Hernantes, J., Sarriegi, J.M.: A holistic framework for building critical infrastructure  
714 resilience. *Technological Forecasting and Social Change*, 103, 21-33, 2016.

715 Liu, H., Meng, Z., Cui S.: A Wireless Sensor Network Prototype for Environmental Monitoring in  
716 Greenhouses", 2007 International Conference on Wireless Communications, Networking and  
717 Mobile Computing, 2007.

718 Lombardi, L., Nocentini, M., Frodella, W., Nolesini, T., Bardi, F., Intrieri, E., Carlà, T., Solari, L.,  
719 Dotta, G., Ferrigno, F., Casagli, N.: The Calatabiano landslide (southern Italy): preliminary GB-  
720 InSAR monitoring data and remote 3D mapping. *Landslides*, 1-12, 2016.

721 Luzi G.: Ground Based SAR Interferometry: a novel tool for geoscience. P. Imperatore, D. Riccio  
722 (Eds.), *Geoscience and Remote Sensing. New Achievements, InTech*, 1-26, 2010. (Available at:  
723 [http://www.intechopen.com/articles/show/title/ground-based-sar-interferometry-a-novel-tool-for-](http://www.intechopen.com/articles/show/title/ground-based-sar-interferometry-a-novel-tool-for-geoscience)  
724 [geoscience](http://www.intechopen.com/articles/show/title/ground-based-sar-interferometry-a-novel-tool-for-geoscience)).

725 Martino, S., Mazzanti, P.: Integrating geomechanical surveys and remote sensing for sea cliff slope  
726 stability analysis: The Mt. Pucci case study (Italy). *Natural Hazards and Earth System Sciences*, 14  
727 (4), 831-848, 2014.

728 Monserrat, O., Crosetto, M., Luzi, G.: A review of ground-based SAR interferometry for  
729 deformation measurement. *ISPRS J Photogramm*, 93, 40–48, 2014,

730 Parthasarathy, A., Chaturvedi, A., Kokane, S., Warty, C., Nema, S.: Transmission of big data over  
731 MANETs. 2015 IEEE Aerospace Conference, 2015.

732 Rudolf, H., Leva, D., Tarchi, D., Sieber, A.J.: A mobile and versatile SAR system. 1999 IGARSS  
733 Proc, Hamburh, 1999.

734 Severin, J., Eberhardt, E., Leoni, L., Fortin, S.: Development and application of a pseudo-3D pit  
735 slope displacement map derived from ground-based radar. *Engineering Geology*, 181, 202-  
736 211,2014.

737 Sirangelo, B., Versace, P., Capparelli, G.: Forewarning model for landslides triggered by rainfall  
738 based on the analysis of historical data file. IAHS-AISH Publication, 278, 298-304, 2003.

739 Snyder, L., Burns, A.A.: Framework for critical infrastructure resilience analysis. Energy and  
740 systems analysis-infrastructure. Sandia National Laboratories, 2009

741 Tapete, D., Casagli, N., Luzi, G., Fanti, R., Gigli, G., Leva D.: Integrating radar and laser-based  
742 remote sensing techniques for monitoring structural deformation of archaeological monuments.  
743 Journal of Archaeological Science, 40(1), 176-189, 2013.

744 Tarchi, D., Ohlmer, E., Sieber, A.J.: Monitoring of structural changes by radar interferometry. Res.  
745 Non Destr. Eval., 9, 213-225, 1997.

746 Tarchi, D., Rudolf, H., Luzi, G., Chiarantini, L., Coppo, P., Sieber, A. J.: SAR interferometry for  
747 structural change detection: a demonstration test on a dam. Proc. of Geoscience and Remote  
748 Sensing Symposium, IGARSS 1999, 3, 1525-1527, 1999.

749 Tarchi, D., Casagli, N., Fanti, R., Leva, D., Luzi, G., Pasuto, A., Pieraccini, M., Silvano, S.:  
750 Landslide monitoring by using ground-based SAR interferometry: an example of application to the  
751 Tessina landslide in Italy. Engineering Geology, 1, 68, 15-30, 2003.

752 Urlainis, A., Shohet, I.M., Levy, R., Ornai, D., Vilnay, O.: Damage in critical infrastructures due to  
753 natural and man-made extreme Events – A critical review. Procedia Engineering, 85, 529-535,  
754 2014.

755 Urlainis, A., Shohet, I.M., Levy, R.: Probabilistic Risk Assessment of Oil and Gas Infrastructures  
756 for Seismic Extreme Events. Procedia Engineering, 123, 590-598, 2015.

757 Venkateswaran, V. and Kennedy, I.: How to sleep, control and transfer data in an energy  
758 constrained wireless sensor network. 2013 51<sup>st</sup> Annual Allerton Conference on Communication,  
759 Control, and Computing (Allerton), 2013.

760 Versace, P., Capparelli, G., Leone, S., Artese, G., Costanzo, S., Corsonello, P., Di Massa, G.,  
761 Mendicino, G., Maletta, D., Muto, F., Senatore, A., Troncone, A., Conte, E., Galletta, D.: LEWIS  
762 project: An integrated system of monitoring, early warning and mitigation of landslides risk.  
763 Rendiconti Online Societa Geologica Italiana, 21(1), 586-587, 2012.

764 Yoo, S., Kim, J., Kim, T., Ahn, S., Sung, J., Kim, D.: A2S: Automated Agriculture System based  
765 on WSN. 2007 IEEE International Symposium on Consumer Electronics, 2007.